Hindawi
International Journal of Photoenergy
Volume 2018, Article ID 8380276, 15 pages
https://doi.org/10.1155/2018/8380276

Research Article

Optimal Design Method of a Hybrid CSP-PV Plant Based on Genetic Algorithm Considering the Operation Strategy

Rongrong Zhai, Ying Chen, Hongtao Liu, Hao Wu, and Yongping Yang

School of Energy, Power and Mechanical Engineering, North China Electric Power University, Beijing 102206, China

Correspondence should be addressed to Rongrong Zhai; zhairongrong01@163.com

Received 1 May 2018; Revised 6 July 2018; Accepted 6 September 2018; Published 6 November 2018

Guest Editor: Mohammad O. Hamdan

Solar energy is the most abundant renewable energy and it has a great potential for development. There are two ways to transfer solar energy to electricity: photovoltaic power generation (PV) and concentrated solar power (CSP). CSP-PV hybrid system can be fully integrated with the advantages of the two systems to achieve low cost, stable output, and manageable to generate electricity. In this paper, the operation strategy of the CSP-PV system is proposed for parabolic trough CSP system and PV system which are now commercially operated. Genetic algorithm is used to optimize the design of the system and calculate PV-installed capacity, battery capacity, and storage capacity of CSP system, making the system to achieve the lowest cost of electricity generation. The results show that the introduction of the CSP system makes it possible to ensure the stability of the output power of hybrid system when the battery capacity is small, which greatly improves the annual utilization time of the PV and reduces solar abandonment. When the system is optimized by operation characteristics of Spring Equinox, the lowest LCOE is 0.0627 $/kWh, the rated capacity of PV and CSP system are 222.462 MW and 30 MW, respectively, and the capacity of heat storage and battery are 356.562 MWh and 14.687 MWh. When the system is optimized by the operation characteristics of the whole year, the lowest LCOE is 0.0555 $/kWh, the rated capacity of PV and CSP system are 242.954 MW and 30 MW, respectively, and the capacity of heat storage and battery are 136.059 MWh and 8.977 MWh. The comparison shows that the power generation curves of the hybrid system are similar in the two optimization-based methods—Spring Equinox based and annual based, but LCOE is lower when optimized by the annual operation characteristic, and the annual utilization rate of the system is higher when optimized by Spring Equinox based.

1. Introduction

Climate change and the scarcity of natural resources make the world to look for a cleaner and more efficient way to use energy to meet the growing energy needs. At present, renewable energy has a great potential and developed rapidly, and it will occupy an important share of future energy structure [1]. However, the major shortcomings of renewable energy are that their variability and intermittency can cause frequent imbalances and serious problems with the grid. The researchers have suggested that different strategies can be used to improve the safety and quality of energy supply, such as the use of more flexible thermal power plants [2], the introduction of appropriate energy storage equipment, and the use of multicomplementary strategy [3].

Solar energy is one of the most abundant renewable resources; solar radiation to reach the Earth's surface is 1800 times as the world's primary energy consumption [4]. There are two ways to convert solar energy into electricity: solar photovoltaic power generation and concentrated solar power [5]. The development of solar photovoltaic power generation is fast, and the ratio of installed solar photovoltaic will reach 16% of the global energy consumption [6]. The power generation costs of photovoltaic systems is relatively lower because of the low price of PV modules, and it can also be achieved grid parity in the absence of any market incentives [6]. However, the high price of photovoltaic energy storage system obstacles the further large-scale application of photovoltaic systems. Many scholars have focused on the concentrated solar power in the recent years; due to that, solar

thermal system can be combined with the thermal storage system, so that the solar power plant can meet the requirements of grid operation and the peak load after the sun can still be deployed [7]. But due to the slow development of technology, the cost of solar thermal system is decreased lower than the solar photovoltaic system [8]. In this context, PV system and CSP system were initially considered to be competitors, but they are complementary in fact. The combination of the two technologies is increasingly concerned. PV-CSP hybrid system is a viable way to generate power, and it can meet the local electricity demand and cost less than a single concentrated solar power [9]. The combination of solar photovoltaic power and solar thermal power can improve the capacity factor of the system and can be dispatched to meet the load demand of peak period [10]. The photovoltaic power is rich and cheap to meet the power load during the day; the peak load in the night will be met by solar thermal power system with storage. Then the stability and schedulability of the system can be ensured at low cost.

At present, a CSP-PV hybrid power system is being built in Ottana of Italy, the system is comprised of a 600 kW linear Fresnel concentrated solar power with 15 MWh heat storage and a 400 kW photovoltaic system with 430 kWh battery. Cocco et al. contrasted the two hybrid ways of the system, which are partially integrated and full-integrated, and found that the annual power generation and annual operating hours of the system on full-integrated were higher [11]. Cau et al. optimized the system's operational strategy by meteorological condition to maximize the annual power generation of the system while meeting the energy conservation and the minimum climbing time [12].

The CSP-PV hybrid system on the Atacama Desert in Chile coupled 20 MW photovoltaic solar system and solar tower power system with 300 MWh storage; the cost of power generation is lower than CSP-alone power system but higher than photovoltaic power system. The levelized cost of electricity (LCOE) in 2014 is 14.69 US cent/kWh and 13.88 cent/kWh, respectively, based on Bluemap and Roadmap [9]. Capacity factor of typical intermittent energy is about 20%–40%, this system can reach about 90% [12]. Green et al. proposed an operation with priority on the basis of this system; the priority of the output power is 50 MW, 100 MW, and 130 MW [13]. Hlusiak et al. found that the collector has the greatest impact on the total cost, followed by coal prices; impacts of photovoltaic capacity and thermal storage system on the cost of power generation is relatively small; the cost of the CSP-PV hybrid system is 13% cheaper than the stand-alone concentrated solar power system with molten salt heat storage [14]. Bootello et al. divided power generation into three grades: the energy consumption of the tracking system, the energy consumption of the auxiliary equipment of the power plant and power generation connected to grid, and put forward the operation mode of the hybrid power station [15]. Larchet found that CSP-PV hybrid system with coal-fired backup unit has the lowest cost of electricity generation and project capital output. LCOE of this system is 42% and 52% lower than PV-alone system and PV-diesel hybrid system, respectively. CSP-PV hybrid system increased the investment but decrease the emission compared to coal-fired power system [16]. The combination of solar thermal and photovoltaic can provide stable energy and increase the capacity factor of the solar thermal power system. It not only can meet the basic requirement of the energy system but also can provide a low-risk investment option [17].

The research on CSP-PV hybrid system are mainly focused on the operation strategy and technical-economic analysis. But the research on the optimal configuration of CSP-PV hybrid system considering the operation strategy is few. In this study, the operation strategy of CSP-PV system is proposed for parabolic trough CSP system and PV system which are now commercially operated. Genetic algorithm is innovatively used to optimize the design of system and calculate PV installed capacity, battery capacity, and storage capacity of CSP system, making the system to achieve the lowest cost of electricity generation. The operation strategy proposed in this paper provides a new idea for the design and operation of CSP-PV hybrid power generation system. The optimization method can be used in the preliminary design of power station.

2. System Description

CSP-PV hybrid power system is composed of concentrated solar power system and photovoltaic system as shown in Figure 1. The upper dashed line box is the photovoltaic power generation subsystem, and the lower dashed box is the concentrated solar power subsystem. The PV power generation system includes PV array, inverter subsystem, and electronic storage system. The PV array consists of a number of subarrays, each of which consists of 20 PV modules with a rated power of 250 W. Each PV subarray is connected to the inverter to ensure that the DC will be converted into AC. At the same time, each inverter is equipped with a maximum power point tracking (MPPT) device to ensure that the photovoltaic subarray can run at the maximum power point. The PV modules are placed south and have a certain tilt angle, which maximizes the annual generation of photovoltaic power generation systems. The PV power generation technology is mature and the system is simple and has flexible layout and low operating costs. However, solar energy resources are fluctuating and intermittent, which makes the output power of photovoltaic power unstable, and it will have great impact on the power grid to a certain extent. To improve the stability of photovoltaic power output, the batteries are configurated.

The CSP system consists of trough collector subsystem, two tanks thermal storage subsystem, and power block subsystem. Heat transfer oil is used as heat transfer fluid, and molten salt is used as the heat storage medium. The inlet temperature of the heat transfer oil is 295°C, and the outlet temperature is 395°C. The feed water is heat by the heat transfer oil to become superheated steam and work in the steam turbine. When solar energy is sufficient, one part of the energy of the collector system is sent into the thermal cycle of power generation, another is storage by molten salt for power cycle when the solar energy is poor. When the stored energy is used out, the gas backup can be started to meet the required load. The concentrated solar power system

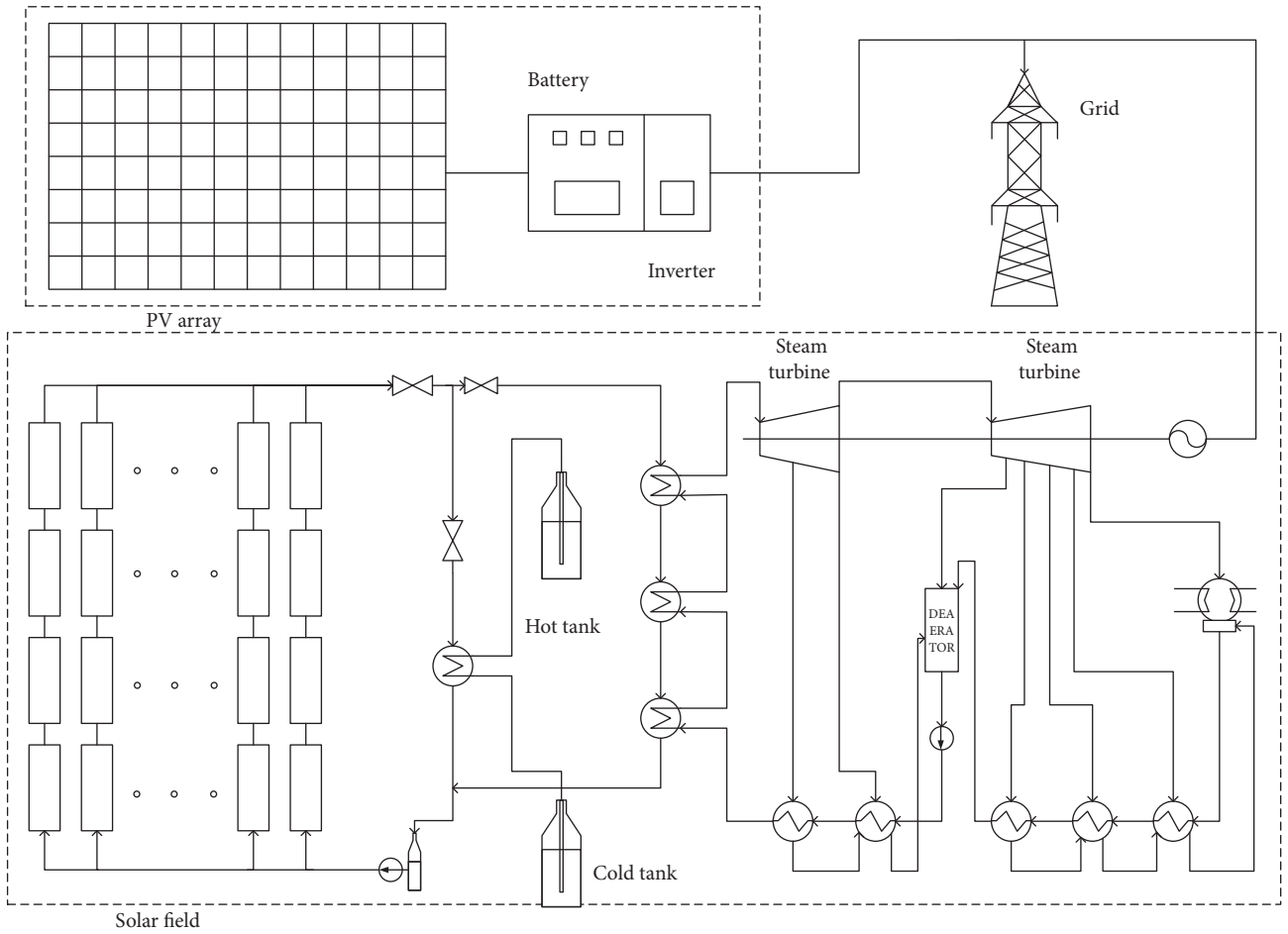

Figure 1: CSP-PV hybrid power system.

adopts the energy conversion form of light-heat-electricity, in which the thermal delay of the system and the heat storage system makes the output power of the concentrated solar power system stable, reduce fluctuation of solar energy, and improve the manageability of renewable energy. Therefore, it is expected that a low-cost manageable output solar power generation system will be established by coupling a low-cost photovoltaic power generation system with a concentrated solar power system that can be used for peaking.

The main parameters that affect the energy and economic performance of the system are the collector field area, the storage capacity, the Rankine cycle power, the PV-installed capacity, and the capacity of the battery. In this paper, based on the 30 MW CSP system, the storage capacity, the PV-installed capacity, and the capacity of the battery are selected as the optimization objects to make the power generation cost of the system minimal.

The main parameters of power block in the design condition are shown in Table 1.

Table 1: Main parameters of power block.

	Pressure (MPa)	Temperature (°C)	Mass flow (kg/s)
Main steam	9.80	369.41	55.8
The first extraction	4.00	257.59	6.8
The second extraction	1.70	204.32	4.4
The third extraction	0.60	250.55	1.9
The fourth extraction	0.25	163.75	1.8
The fifth extraction	0.12	104.78	1.4
The sixth extraction	0.06	85.93	2.6
Exhaust steam	0.008	41.51	36.9

3. Model Establishment

Performance analysis of CSP-PV hybrid power system is realized in software Matlab [18]. The simulation model has been simplified. The collector field area, the heat storage capacity, the Rankine cycle power, the PV-installed capacity, and the capacity of the battery are the main design parameters that affect the system performance. The design of the system is optimized in order to find the system structure with the lowest cost of power generation under

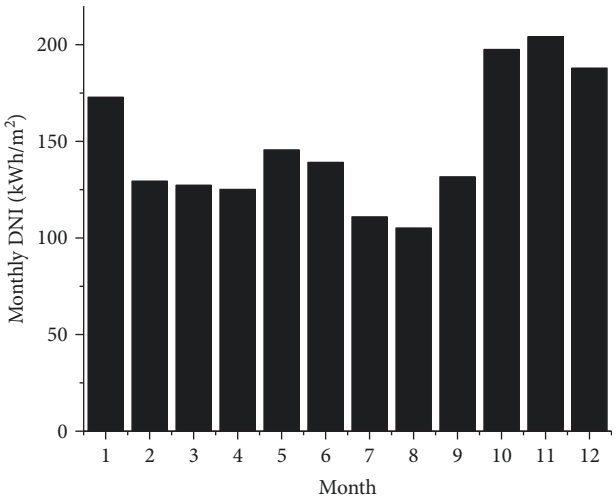

Figure 2: Monthly DNI of Lhasa.

the constraints of energy balance and storage energy. The CSP-PV hybrid system model includes the photovoltaic subsystem model and the solar thermal subsystem model. The input parameters of the model are the meteorological data of a certain location.

3.1. Solar Energy Resources. In this paper, the database of a typical meteorological year is from SAM software [19] and Lhasa (91.13°E 29.67°N) is selected. In this paper, the database of a typical meteorological year is from NREL [20]. The meteorological data include direct normal irradiation (DNI), global horizontal irradiance (GHI), ambient temperature, and wind speed.

Annual DNI and GHI of Lhasa are 1777 kWh/m^2 and 1818 kWh/m^2, respectively. In Lhasa, the annual variation of GHI is small and the radiation intensity is large, but DNI varies greatly with season changes and the radiation intensity of autumn and winter is higher than that of summer. The variation of solar radiation intensity makes the performance of the system change greatly. Monthly DNI of Lhasa is shown in Figure 2.

3.2. PV Subsystem Model. The PV system model consists of photovoltaic panels which output is rated at 250 W. PV panels are placed at a fixed angle and faced south. According to the equation proposed by Duffle, the effect of PV module temperature change on the power generation performance of the system is considered.

The main parameters of PV panels are shown in Table 2. The operating temperature (T_C) of PV panels is determined by the rated operating temperature of PV panels (equation (1)).

$$T_C = T_A + (T_{\mathrm{NOCT}} - T_{A,\mathrm{NOCT}}) \frac{\mathrm{GI}}{\mathrm{GI}_{\mathrm{NOCT}}} \frac{U_{L,\mathrm{NOCT}}}{U_L} \left[1 - \frac{\eta_{\mathrm{PV}}}{\tau\alpha}\right], \tag{1}$$

where T_A is the ambient temperature; the ambient temperatures for nominal operating cell temperature ($T_{A,\mathrm{NOCT}}$) is 20 °C; the solar radiation ($\mathrm{GI}_{\mathrm{NOCT}}$) is 800 W/m^2; U_L and $U_{L,\mathrm{NOCT}}$ is the actual and rated heat transfer factor; η_{PV} is the actual PV panel efficiency, which can be calculated by equation (2). $\tau\alpha$ is the transfer absorption factor [21]. The efficiency of PV panels

Table 2: Main parameters of PV module.

PV module		Other assumptions	
Solar cell technology	Polycrystalline	Derating factor f_{PV}	0.8
Nominal power $P_{\mathrm{PV,REF}}$	250 W	$U_{L,\mathrm{NOCT}}$	9.5
Nominal efficiency $\eta_{\mathrm{PV,NOM}}$	14.9%	U_L	$5.7 + 3.8\,V_{\mathrm{wind}}$
Nominal operating cell temperature T_{NOCT}	46°C	Transmittance-absorptance coeff. ($\tau\alpha$)	0.8
Active panel area A_{MOD}	1.675 m^2	Inverter nominal efficiency	97.8%
Temperature coeff. of power γ	−0.41%/K	Nominal global irradiance $\mathrm{GI}_{\mathrm{NOCT}}$	800 W/m^2

$$\eta_{\mathrm{PV}} = \eta_{\mathrm{PV,NOM}}[1 + \gamma(T_C - T_{C,\mathrm{REF}})], \tag{2}$$

where $\eta_{\mathrm{PV,NOM}}$ is the nominal efficiency; γ is the temperature factor; $T_{C,\mathrm{REF}}$ is the PV module temperature under standard test conditions (25°C).

$$P_{\mathrm{PV}} = n_{\mathrm{MOD}} A_{\mathrm{MOD}} GI \eta_{\mathrm{PV}} \eta_{\mathrm{INV}} f_{\mathrm{PV}}. \tag{3}$$

The output power of PV panels can be calculated using equation (3). Where n_{MOD} is the number of PV subarray; A_{MOD} is the active area of each PV module, and η_{INV} is the inverter efficiency. A derating factor f_{PV} is finally considered to account for soiling of the panels, wiring losses, shading, snow cover, aging, and other secondary losses.

The use of batteries can make up for difference between PV power generation and energy demand. The energy available for the battery can be described as the charge state "SOC_B", which is the ratio of the stored energy to the rated storage capacity. The battery model can be calculated by the following formula. Where η_{BC} and η_{BD} are the battery efficiencies during charge and discharge processes, respectively. Battery efficiency depends on several operating parameters such as current, SOC, charging and discharging power, and battery lifetime. To simplify the model, a constant efficiency of 94% is assumed as declared by the manufacturer while a nominal Depth-of-discharge (DOD) of 80% is considered (with a minimum SOC of 10% and a maximum SOC of 90%).

$$\mathrm{SOC}_B(t) = \mathrm{SOC}_B(t-1) + \frac{(P_{\mathrm{BC}}\eta_{\mathrm{BC}} - (P_{\mathrm{BD}}/\eta_{\mathrm{BD}}))\Delta t}{E_B}. \tag{4}$$

Table 3: Main parameters of CSP module.

Design condition		Optical coefficient	0.98
DNI	800 W/m^2	Reflectance efficiency	0.93
Ambient temperature	3°C	Cleanliness factor	0.95
Trough collector		Tracking factor	0.99
Focal length	1.84 m	Dust cover coefficient	0.98
Width	5 m	End shadow coefficient	0.97
Unit length	8 m	Transmissivity factor	0.96
Oil inlet/outlet temp.	285/390°C	Coating absorption factor	0.95
		Other factor	0.96

Table 4: Physical property of solar salt.

Melting point	220°C	Viscosity	1.776 cP
Ceiling temperature	600°C	Thermal conductivity	0.519 W/(m·K)
Surface tension	109.2 mN/m	Thermal capacity	1495 J/(kg·K)
Density	1837 kg/m^3	Fusion heat	161 kJ/kg

The PV model is established based on the literature [22]. Rated output power is 30000 kW. The annual power generation of Matlab model is 130690 MWh. The plant electricity rate is defined as the electricity consumed by the power plant itself divided by the gross electricity produced by the power plant. The plant electricity rate is assumed as 2.43% according to statistics of Chinese power generation, then the actual power generation is 127514 MWh. The annual power generation of SAM is 122179 MWh, and the deviation of annual power generation is 4.18%. The reason for the higher power generation in Matlab is that the model ignores few losses of the actual power generation process.

3.3. CSP Subsystem Model. The simulation of the CSP generation system is based on the parameters of the 30 MW SEGS VI CSP plant.

The solar input is determined by equation (5):

$$Q_{\text{solar}} = \text{DNI} \cdot A_{\text{net}} \cdot \text{KIA} \cdot f_{\text{opt}} \cdot f_{\text{ref}} \cdot f_{\text{trac}} \cdot f_{\text{end}} \cdot f_{\text{clean}} \cdot f_{\text{dust}} \cdot f_{\text{tran}} \cdot f_{\text{abs}}, \quad (5)$$

where A_{net} is the net aperture area of parabolic trough collector, KIA is incident angle correction, f_{opt} is the optical coefficient, f_{ref} is the reflectance efficiency, f_{trac} is the tracking factor, f_{end} is the coefficient to correct end loss effects, f_{clean} is the factor to correct for actual mirror cleanliness, f_{dust} is the factor to correct for dust cover, f_{tran} is the transmissivity factor, and f_{abs} is the coating absorption factor.

The main parameters of the CSP station are shown in Table 3 [22]. The hourly operating characteristics analysis of CSP system is based on the meteorological conditions, especially solar radiation and solar location. The heat loss of the collector field is taken into account. The Equinox day of Lhasa, annual average DNI, and annual average temperature is selected as the system design point.

LS-2 collector tube is used as solar collectors, and the row space is 15 m. The heat loss of the collector is affected by DNI, flow of heat transfer oil, ambient temperature, and wind speed. Usually, the impact of wind speed on heat loss can be ignored.

The available heat input depends on the solar heat input, the thermal losses of the receivers, and the field piping, as shown in equations (6) and (7) [23], where T_{i} and T_{O} are the inlet and outlet temperature of the heat transfer oil. The heat pipe is composed of a loop, and each circuit is connected through a pipe. The heat loss on the pipe is obtained from the empirical formula (8) [23], where ΔT is the temperature difference between the average temperature of the collector field and the ambient temperature.

$$Q_{\text{avail}} = Q_{\text{solar}} - Q_{\text{col,loss}} - Q_{\text{pipe}}, \quad (6)$$

$$Q_{\text{col,loss}} = \frac{a_0(T_0 - T_i) + (a_1/2)\left(T_0^2 - T_i^2\right) + (a_2/3)\left(T_0^3 - T_i^3\right) + (a_3/4)\left(T_0^4 - T_i^4\right)}{T_0 - T_i} + \frac{\text{DNI}\left[b_0(T_0 - T_i) + (b_1/3)\left(T_0^3 - T_i^3\right)\right]}{T_0 - T_i}, \quad (7)$$

$$Q_{\text{pipe}} = 0.01693\Delta T - 0.0001683\Delta T^2 + 6.78 \times 10^{-7}\Delta T^3. \quad (8)$$

The heat storage medium of CSP system is binary molten salt, which composes of 60% $NaNO_3$ and 40% KNO_3, and the physical properties are shown in Table 4 [24]. The available energy of the heat storage is obtained by the energy balance of the collector field, the power block, and the heat loss. In this paper, the heat loss of the thermal storage tank is assumed to be 2%. The thermal oil VP-1 is used for heat transfer fluid, which has a wide optimum use range of 12° to 400°C.

The solar thermal energy absorbed by the collectors is stored in the thermal storage system as thermal energy. When the power output from CSP subsystem is needed, the molten salt releases heat and water is heated and turned into steam, making the turbine work. The turbine efficiency is variable and related to the steam mass flow in the off-design condition. Variation of turbine efficiency under off-design conditions is considered in power block model. The reduction rate in turbine efficiency can be calculated using

equation (9) [25], then turbine efficiency can be calculated using equation (10). The generator efficiency can be calculated using equation (11) [26].

$$\text{Reduction rate} = 0.191 - 0.409\frac{m}{m_{\text{ref}}} + 0.218\left(\frac{m}{m_{\text{ref}}}\right)^2, \quad (9)$$

$$\eta = (1 - \text{Reduction rate})\eta_{\text{ref}}, \quad (10)$$

$$\eta_{\text{generation}} = 0.9 + 0.258\text{load} - 0.3\text{load}^2 + 0.12\text{load}^3. \quad (11)$$

The CSP model is established based on the literature [19] and is compared to SAM software simulation results. The annual power generation of the model is 66584.75 MWh, the plant electricity rate is assumed as 5%; then, the actual power generation is 63255.5 MWh. The annual power generation of SAM is 61167.6 MWh, and the deviation of annual power generation is 3.3%. The main reason is that this model is simplified that some of the error is ignored, making the model of the annual power generation higher.

4. Methodology

4.1. Operation Strategy. Operation strategies of the system can be divided into two modes: prioritize the PV (mode 1) and minimize the turbine shutdown (mode 2). Using mode 1, the PV and the battery is prioritized over the CSP. That is to say that if the PV capacity is large enough to cover the load, it does and the CSP is shut down. The same can be said for the battery, if the battery discharge capacity is large enough to cover the load, it does and the CSP is shut down for the period that the battery discharges. This mode of operation will make the operation and maintenance costs of the system increase and the operating life decrease. However, the CSP must be shut down only if it remains offline for a sufficient amount of time. A turbine hot start can take as long as 1–2 hours. Therefore, in mode 2, the CSP plant will be shut down if it should be shut down for more than 2 hours.

The operation strategy was proposed by combining two modes and was shown in Figure 3. Where $W_{\text{min,turb}}$ is the minimum output of turbine, W_{set} is the rated output of the hybrid system, W_{CSP} and W_{PV} are the real output of CSP system and PV system, respectively, sto and BESS are the energy stored in the storage tank of CSP system and in the battery of PV system, respectively.

There are three operation modes according to the operation strategy.

(1) Energy of PV panels can meet energy demand and PV system runs alone. Exceeded energy is stored in a battery and the collected energy of CSP system is all stored in a storage tank

(2) Energy of PV panels cannot meet energy demand, and PV panels and battery are both used for energy generation. The collected energy of CSP system is all stored in a storage tank

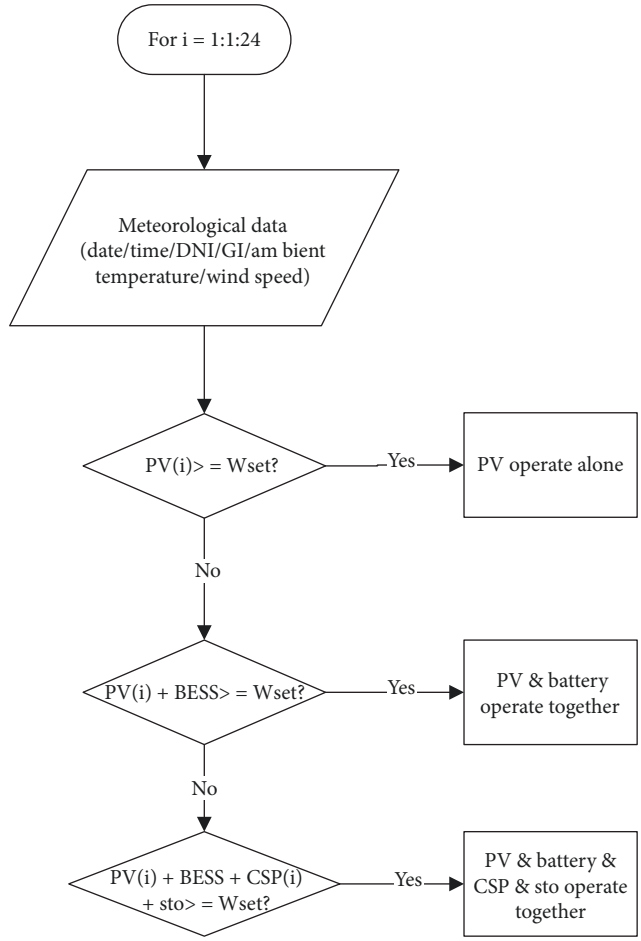

Figure 3: Operation strategy of CSP-PV hybrid power system.

(3) Energy of PV panels and battery cannot meet energy demand, and PV panels, battery, CSP system, and storage tank are all used for energy generation

4.2. Method of Optimization. Method of optimization adopted in this study is genetic algorithm. The classical optimization algorithm such as linear program and dynamic programming is easy to fall into the local optimal, and it is difficult to solve the global optimal problem. Genetic algorithm is a good way to overcome this shortcoming and is a global optimization algorithm with good convergence. Many scholars use genetic algorithms to optimize the system. The genetic algorithm is used to optimize the heat recovery system of the rotary kiln, and the mathematical relationship between the design parameters and the temperature and heat transfer rate of the heat recovery switch is deduced. The total heat transfer area and the total power consumption is reduced [27]. Gentils et al. optimized the support structure for offshore wind power, along the outer diameter and cross-sectional thickness of the support structure selected as the design variable. Optimizing makes the quality of the support structure reduced by 19.8% [28]. Li et al. used the reservoir as a decision variable to minimize the variance of the power output and maximize the annual power generation which is a goal by the NSGA-II [29].

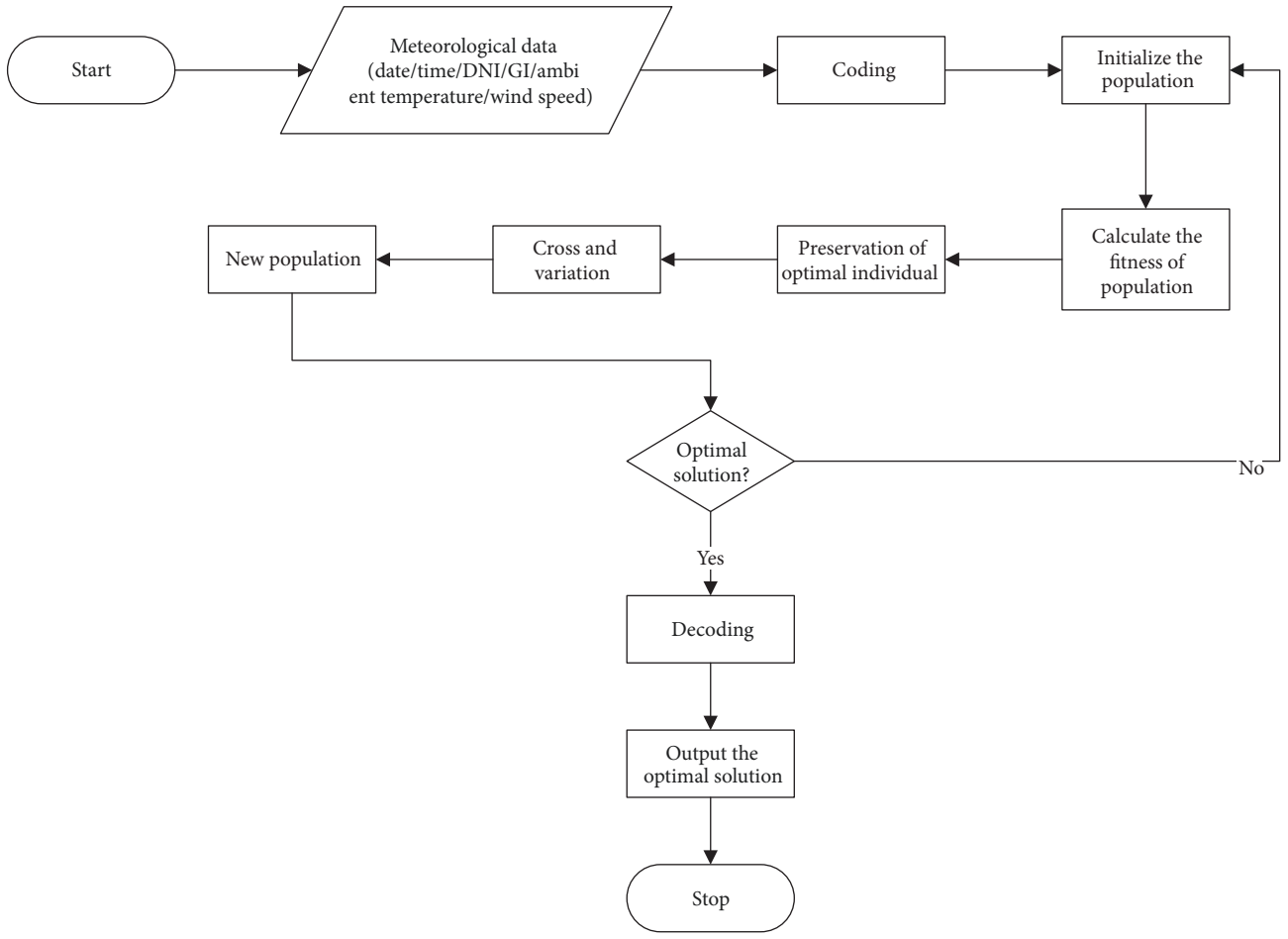

Figure 4: Process of genetic algorithm.

Genetic algorithm is an optimization method that simulated biological evolution. It is based on the principle of biological evolution and strategy of group optimization through iterative calculation of selection, replication, crossover, mutation, insertion, and migration. It is suitable for solving complex optimization problems [30]. The process of genetic algorithm is shown in Figure 4.

The process of genetic algorithm is as follows:

(a) Randomly generate the initial population of the determined length

(b) Calculate the fitness value of the population iterations and produce the next generation of groups through replication, crossover, and mutation

(c) The best individual in each generation as the result of the implementation of the algorithm

(d) After a given genetic algebra, compare all the results of the implementation to obtain the optimal solution as an optimal process

The fitness function chosen in this paper is LCOE (levelized cost of energy). LCOE is calculated by equation (12) [31]. Where IC_{CSP} and IC_{PV} are the initial investment of CSP power station and PV station, respectively, AC_{CSP} and AC_{PV} are the annual cost of CSP power station and PV station, respectively (operation and maintain cost is included), E_{CSP} and E_{PV} are the output power of CSP system and PV system in the first year, d_{CSP} and d_{PV} are annual decay rate of power generation, i is the interest rate, and N is the lifetime of the system.

$$\mathrm{LCOE} = \frac{\mathrm{IC}_{\mathrm{CSP}} + \sum_{n=1}^{N}\left(\mathrm{AC}_{\mathrm{CSP}}/(1+i)^n\right) + \mathrm{IC}_{\mathrm{PV}} + \sum_{n=1}^{N}\left(\mathrm{AC}_{\mathrm{PV}}/(1+i)^n\right)}{\sum_{n=1}^{N}\left(\left(E_{\mathrm{CSP}}(1-d_{\mathrm{CSP}})^n + E_{\mathrm{PV}}(1-d_{\mathrm{PV}})^n\right)/(1+i)^n\right)}, \tag{12}$$

where IC_{CSP} and IC_{PV} can be divided into two parts: direct cost and indirect cost. The direct component is the investment associated with the power block (C_{PB}), solar field (C_{SF}), piping (C_{PIP}), storage system (C_{TES}), salt purchase (C_{SALT}), and balance of plant ($C_{CSP,BoP}$). The indirect component covers all the remaining costs for the upfront investment that are not directly related to the equipment. These costs include the purchase of land (C_{LAND}) and the engineering, procurement, and construction costs (C_{EPC},

Table 5: Cost estimation of the CSP plant and PV system.

CSP direct cost		CSP annual cost	
Solar field cost (C_{SF})	240 \$/m^2 of collector area	O&M annual cost	1.5%
Piping cost (C_{PIP})	36 \$/m^2 of collector area	Insurance annual cost	0.5%
Tank cost (C_{TES})	750 \$/m^3 of storage volume	PV annual cost	
BoP cost ($C_{CSP,BoP}$)	300 \$/kW$_e$	O&M annual cost	1.5%
PV direct cost		Insurance annual cost	0.25%
Panel cost (C_{PV})	1200 \$/kW$_p$	CSP/PV indirect cost	
Inverter cost (C_{INV})	240 \$/kW	Land cost (C_{LAND})	12 \$/m^2
BoP cost ($C_{pv,BoP}$)	240 \$/kW	Engineering cost (C_{EPC})	20%
Battery cost (C_B)	1200 \$/kWh	Other assumption	
PV degradation rate	0.6%	Annual interest rate	7%
Operating lifetime	25 years	CSP degradation rate	0.2%

Table 6: Optimization design variables and range.

Variable	Range	Unit
Rated power of photovoltaic plant	0–100	MW
Capacity of heat storage	0–2000	MWh
Capacity of battery bank	0–2000	MWh

calculated as a percentage of the direct costs). The equations for the direct and indirect initial costs of the CSP section are therefore given by

$$\begin{aligned}
IC_{CSP} &= IC_{CSP,DIR} + IC_{CSP,IND},\\
IC_{PV} &= IC_{PV,DIR} + IC_{PV,IND},\\
IC_{CSP,DIR} &= [(C_{SF} + C_{PIP})A_{SF} + (C_{TES} + C_{SALT}\rho_{SALT})V_{TES}]\\
&\quad + (C_{PB} + C_{CSP,BoP})P_{ORC,nom},\\
IC_{CSP,IND} &= C_{LAND}A_{LAND,CSP} + IC_{CSP,DIR}C_{EPC},\\
IC_{PV,DIR} &= [(C_{PV} + C_{INV} + C_{PV,BoP})P_{PV,nom} + C_BE_B],\\
IC_{PV,IND} &= C_{LAND}A_{LAND,PV} + IC_{PV,DIR}C_{EPC}.
\end{aligned} \tag{13}$$

The main economic data is shown in Table 5 [21]. The floor area of CSP power station and PV power station are estimated by literature [32]. The floor area of the PV station whose output is over 20 MW and track by the fixed axis is 7.5 acres/MW, and the floor area of the CSP station is 10 acres/MW.

5. Case Study

The model is established in Matlab and it can simulate the operating performance of CSP-PV hybrid system. The output power of the CSP power station selected in this study is 30 MW. Input parameters are heat storage capacity, nominal power of PV station, and battery capacity, and output parameters are the output power of a hybrid system and LCOE. Then the model can simulate the daily, monthly, and annual performance of a hybrid system. The output power is 95% of the sum of the nominal power of the CSP and PV station. There is a 5% unmet load demand [21].

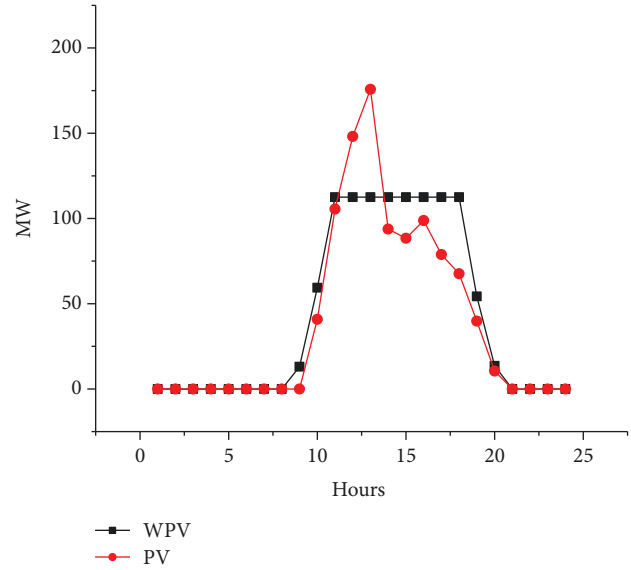

Figure 5: Comparison between the power generation capacity of PV system and the actual power generation on Equinox Day.

The objective function of optimization is LCOE and variable and their range are shown in Table 6.

5.1. Optimization Based on a Typical Day. Optimization is based on the operation characteristics of Equinox Day. According to the results of genetic algorithm, when the installed capacity of the CSP power system is 30 MW, the LCOE of the CSP-PV hybrid system reaches the lowest which is 0.0660 \$/kWh under the condition that the rated power capacity of PV is 222.462 MW, the battery capacity is 14.687 MWh, and the heat storage capacity is 356.562 MWh.

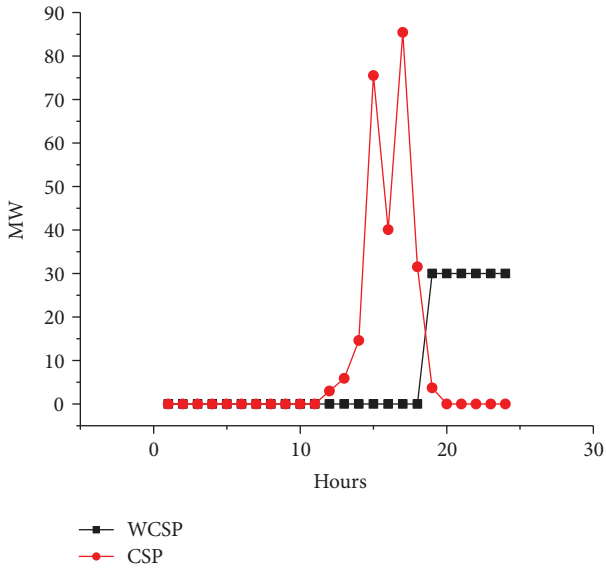

Figure 6: Comparison between the power generation capacity of CSP system and the actual power generation on Equinox Day.

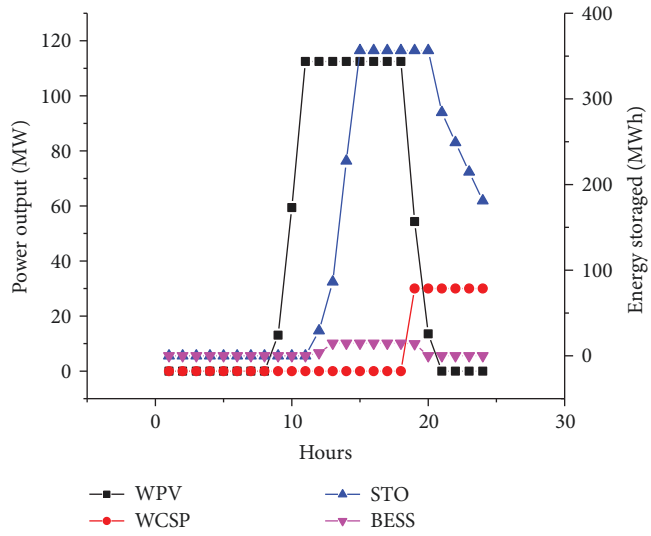

Figure 7: The system output power of Equinox Day of Equinox Day Optimization.

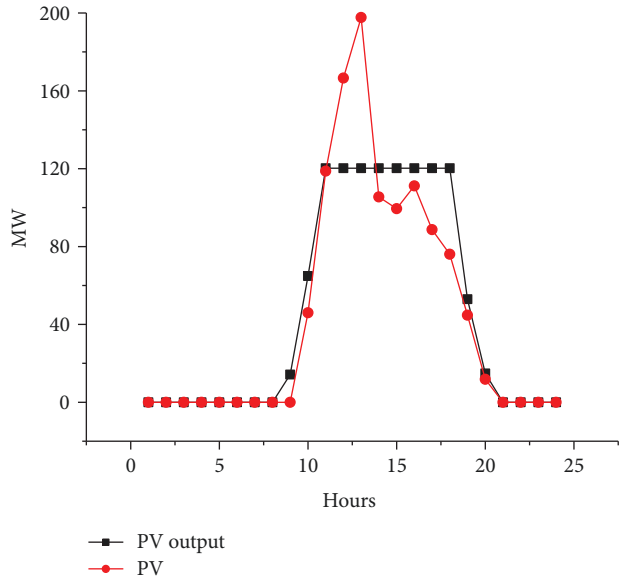

Figure 8: Comparison between the power generation capacity of PV system and the actual power generation on Equinox Day.

Figures 5 and 6 show the comparison between the power generation capacity of PV and concentrated solar power (PV/CSP) and the actual power generation (WPV/WCSP) in Equinox Day. The "PV" represents the power generated by the PV panels, and "WPV" represents the power output from the PV system after dispatch. The "CSP" represents the concentrated solar power energy, and it is stored in the TES. The "WCSP" is the actual power output from a solar thermal Rankine cycle. This is added in the manuscript. After the sun rises, the output power of the PV system increases as the irradiation intensity increases and reaches the maximum at 11 o'clock. The use of the battery makes the output power of the PV power plant does not change with the solar radiation changes, and the power generation curve tends to be gentle which makes the impact of PV system to reduce the power grid small and ensure that the system can still maintain the rated output power when the solar radiation is reduced. The CSP system generates power after 19 o'clock and maintains the rated power output. The use of the thermal storage system allows CSP system to continue to generate electricity after the sun goes down.

The system output power of Equinox Day is shown in Figure 7. After the sun rises, the output power of the PV system increases with the increase of solar radiation. The solar radiation intensity is the largest between 11:00 and 18:00, and the operating mode of the system is the power generated by the PV system alone; exceeded energy from the PV system is stored in the battery and the energy of CSP system is all stored in the heat storage tank. At 19 o'clock, the solar radiation is insufficient, the system operating mode changes from the PV alone into a PV system, the battery system and CSP system generate power at the same time, and the excess heat is stored in the thermal storage system. When at 20 o'clock, the sun is completely down without solar radiation, PV and CSP system has no energy source, then the system operating mode was changed into heat storage that generates power alone. In the system, the power of CSP is used to make up the power generation of the PV system, and the output power of CSP system varies with the PV output power. The more stable PV output power curve is makes the response of CSP system better. The use of heat storage in the CSP system allows the CSP system to continue to generate electricity after the sun goes down and to compensate for the lack of power generation in the PV system without solar radiation.

According to the calculation results, annual power generation of CSP-PV hybrid system is 368722 MWh. Where annual power generation of PV system is 288291 MWh, annual utilization hours are 3261 h which is higher than PV-alone system. Annual power generation of CSP system

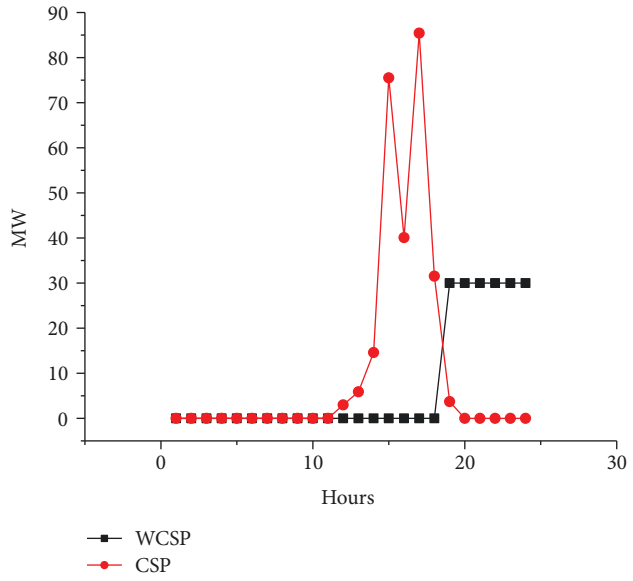

Figure 9: Comparison between the power generation capacity of CSP system and the actual power generation on Equinox Day.

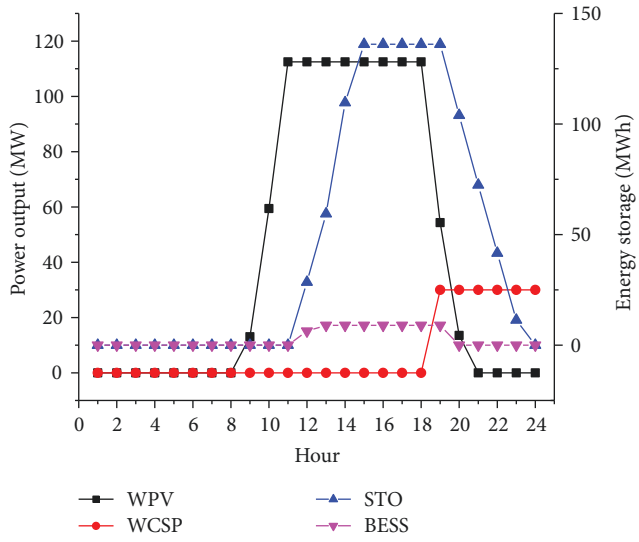

Figure 10: Output power of the system on Equinox Day of whole year optimization.

is 80431 MWh; annual utilization hours are 2681 h which is lower than the 280 MW solar parabolic thermal power system in Solana; the reason is that the storage hour of Solana is 6 hours and the solar radiation is better. The optimized CSP-PV system combines the advantages of the PV power generation and CSP power generation system, which makes the annual operation hours of the PV system increase and the stability of the PV system operation improve, but the LCOE of the system is only 0.0660 $/KWh, which is lower than the CSP power generation alone.

5.2. Optimization Based on the Whole Year. GHI of Lhasa changes slowly with the seasons, and the DNI in summer

Table 7: Comparison between annual and day optimization.

	Optimized by day operation	Optimized by annual operation
Annual output power (MWh)	368722	375695
LCOE ($/kWh)	0.0660	0.0555
CSP		
Capacity of heat storage (MWh)	356.562	136.059
Annual output power of CSP system (MWh)	80431	66659
Annual utilization hours of CSP system (h)	2681	2222
PV		
Installed capacity of PV system (MW)	222.462 MW	242.954
Capacity of battery (MWh)	14.687	8.977
Annual output power of PV system (MWh)	288291	309036
Annual utilization hours of PV system (h)	3261	3201

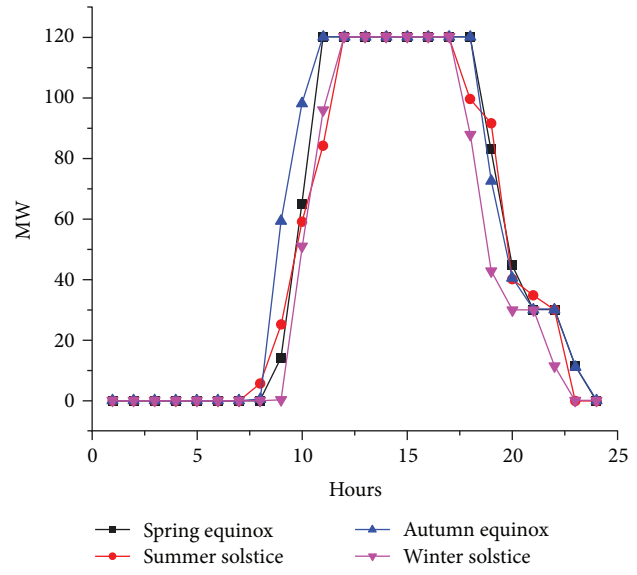

Figure 11: Comparative analysis of four typical days of whole year optimization.

and autumn is higher. To optimize the annual operating characteristics of the system based on the operation strategy proposed above. According to the results of genetic algorithm, when the installed capacity of the CSP power system is 30 MW, the LCOE of the CSP-PV hybrid system reaches the lowest which is 0.0555 $/kWh under the condition that the rated power capacity of PV is 242.954 MW, the battery capacity is 8.977 MWh, and the heat storage capacity is 136.059 MWh. The LCOE is lower compared to

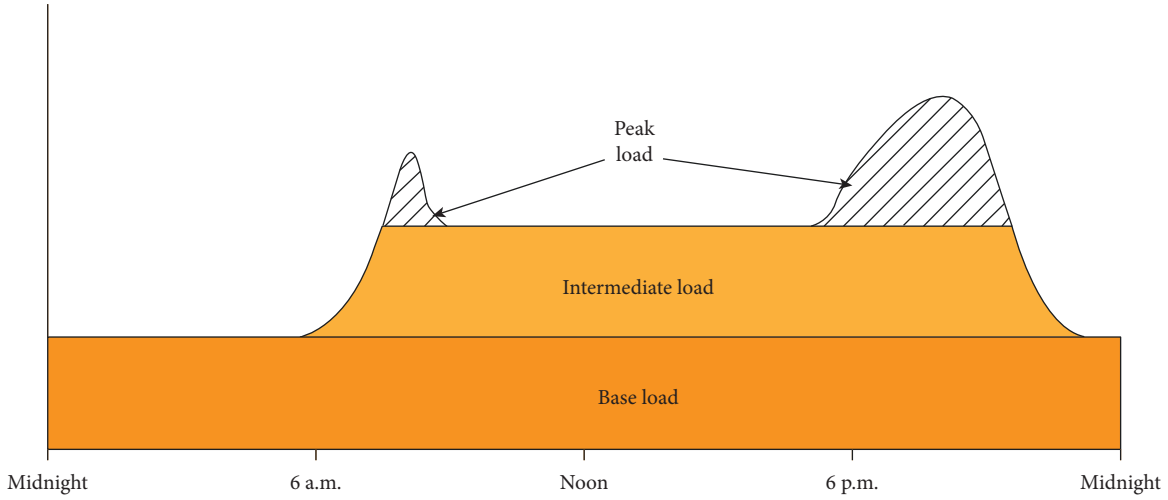

Figure 12: Electricity load curve.

Table 8: Impact of rated output power on CSP-PV system.

	85%	90%	95%	100%
Annual output power (MWh)	328957	399050	375695	384810
LCOE ($/kWh)	0.0592	0.0561	0.0555	0.0530
CSP				
Capacity of heat storage (MWh)	145.613	254.971	136.059	166.577
Annual output power of CSP system (MWh)	69925	80329	66659	74099
Annual utilization hours of CSP system (h)	2331	2678	2222	2470
PV				
Installed capacity of PV system (MW)	78.423	99.805	242.954	97.555
Capacity of battery (MWh)	10.061	11.274	8.977	5.752
Annual output power of PV system (MWh)	259032	318721	309036	310711
Annual utilization hours of PV system (h)	3303	3193	3201	3185

the CSP power generation alone and lower compared to the PV power generation with battery which is to ensure stability of the power output of the system.

It can be found in Figures 8 and 9 from the comparative analysis of the power generation capacity and actual power generation that the output power of PV increases with the increase of solar radiation and reaches the rated output power at 11 o'clock when the system output power is no longer changing with the increase of solar radiation. After 14 o'clock, the solar radiation drops, the PV system still maintains the rated output power, and the application of the battery makes the output power fluctuation of the PV system lower. CSP system does not participate in the system power generation in the daytime and generates electricity after 19:00. Heat storage tank makes the CSP system ensure stable power generation when the sun goes down or no sun irradiation.

The output power of the system in Equinox Day is shown in Figure 10. After the sun rises, the storage tank begins to store energy and the battery stores the excess energy of the PV system. The operation mode of the system that PV operates alone from 11:00 to 18:00 and the exceeded energy is stored in a battery and heat storage tank. When at 19:00, the energy of the PV system is not enough to meet the energy needs, and the system operating mode is converted into the PV, battery, and CSP systems that operate at the same time. After 20:00, the sun has been down the mountain and the battery and the PV system cannot provide energy, then the power is provided by the heat storage tank.

According to the calculation results, annual power generation of the CSP-PV hybrid system is 375695 MWh. Where annual power generation of PV system is 309036 MWh, annual utilization hours are 3201 h which is higher than the PV-alone system. Annual power generation of the CSP system is 66659 MWh; annual utilization hours are 2222 h. It can be found that the use of CSP-PV hybrid system, which CSP system is to make up for the output power fluctuations of PV systems, can be combined with the advantages of both systems to increase annual operating hours of PV systems to reduce the rate of discards and decrease LCOE of the system but also can guarantee stable output.

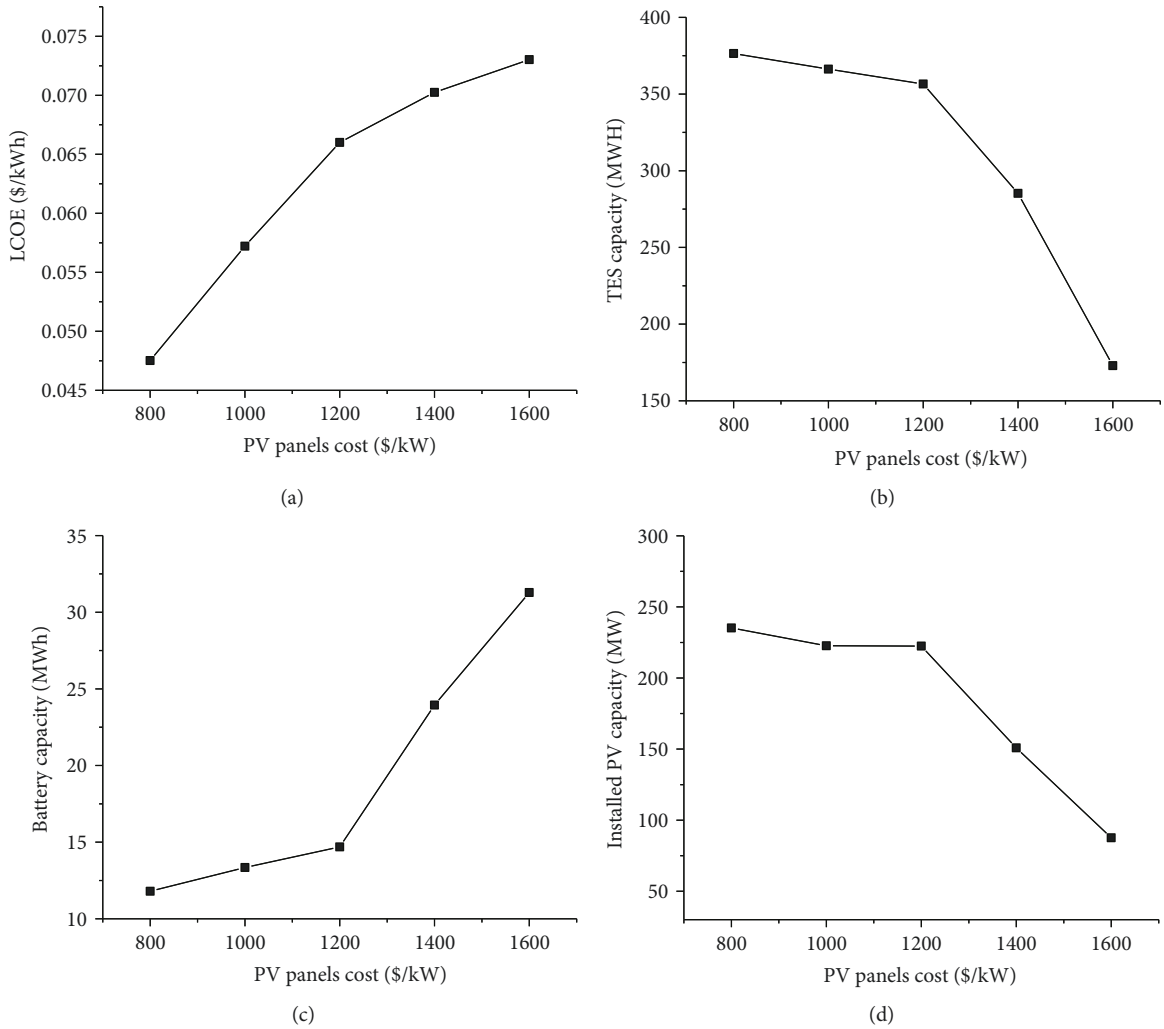

Figure 13: Influence of PV panels cost.

5.3. Discussion. The results of annual and day optimization are shown in Table 7. According to the comparison that can be found, the annual power generation of the system which is optimized by the annual operation characteristic is higher and the LCOE is lower. Annual utilization hours of PV and CSP system is lower due to the lower capacity of battery and heat storage tank which makes solar energy abandon more.

The comparative results of optimization of day and year which includes four typical days: Spring Equinox, Summer Solstice, Autumnal Equinox, and Winter Solstice are shown in Figure 11. It can be seen that the power generation curves of four typical days are basically the same. However, the power generation of Equinox Day is the worst because the solar radiation is poor, and Autumn Day is the best. Therefore, the system optimized with Equinox Day requires more energy storage system and more power generation, but LCOE is also higher in the meantime. The use of optimized CSP-PV system is to generate power at full load in the peak time. This system can be used for intermittent energy power generation compared to the load curve shown in Figure 12.

The estimated gross to net conversion factor, which means the ratio of on-grid electricity to the generated electricity, influences the results greatly. The estimated gross to net conversion factor is set to be from 85% to 100%, and the results are shown in Table 8.

As the estimated gross to net conversion factor increases, the annual output power and LCOE of the system are improved. When the annual operating characteristics are optimized, with the increase of the output power, LCOE of the system is reduced. The main reason is that the battery capacity is reduced. The impact of battery capacity on the system is great. The decrease in battery capacity has reduced the number of utilization hours of PV, but it has little effect.

5.4. Sensitivity Analysis. The influence of PV panels cost and the thermal storage cost based on the Spring Equinox are analyzed. The PV panels cost is varied from 800 $/kW to

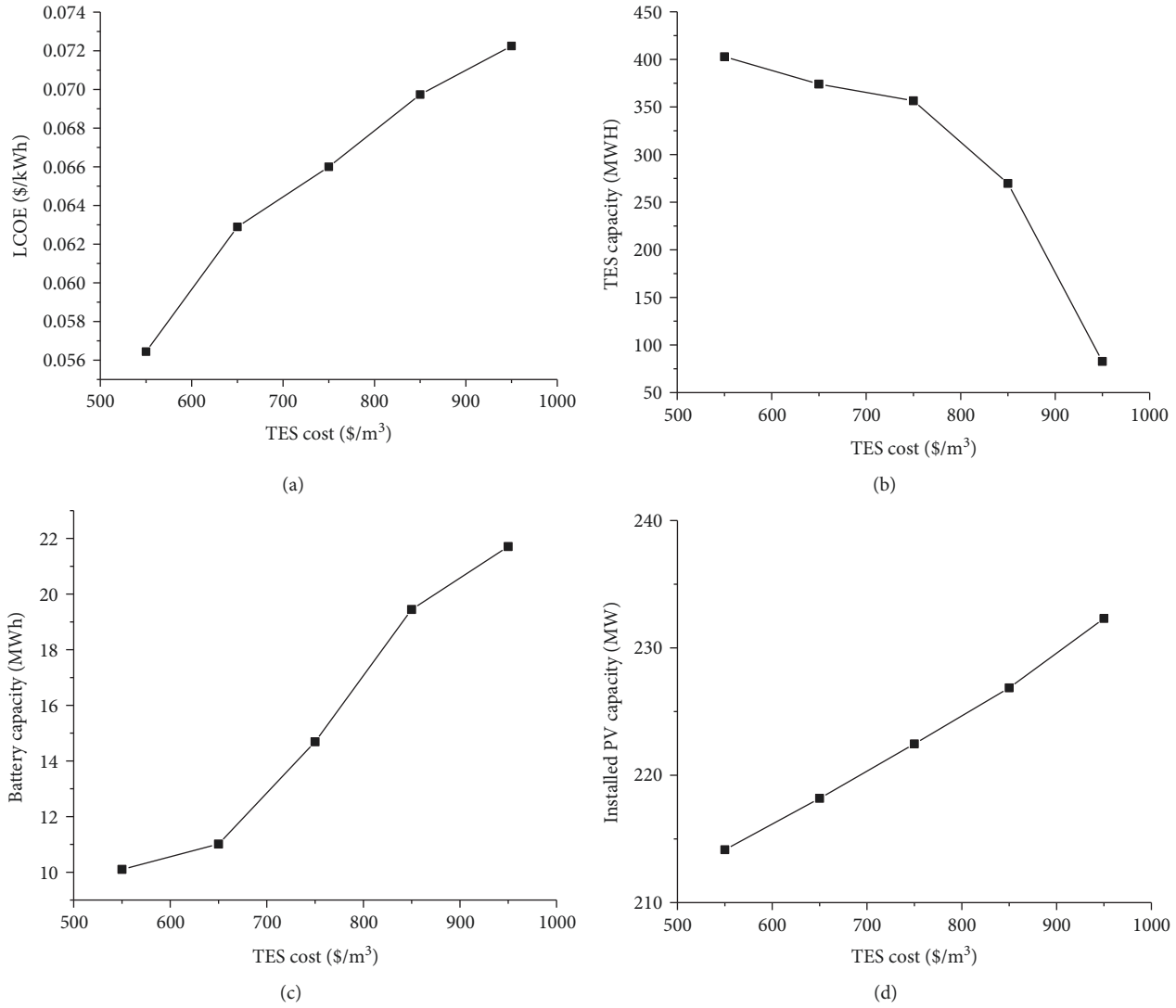

Figure 14: Influence of TES cost.

1600 $/kW, and the thermal storage cost varied from 550 $/m^3 to 950 $/m^3. The results are shown in Figures 13 and 14.

6. Conclusion

In this paper, the operation strategy of CSP-PV hybrid system is proposed. Based on this operation strategy, the ratio of PV and CSP in the system is optimized by genetic algorithm, which makes LCOE of the system to a minimum. Through the calculation of this paper, it is found that the increase of PV capacity in the CSP-PV system can reduce the power generation cost of the system; the cost of the battery is high and when the use of batteries will greatly improve the power generation cost of the system; the introduction of the CSP system makes it easy to ensure the stability of the output power of the system in the case of small battery capacity, which greatly improves the annual utilization of the PV and reduces the number of solar discard, but to a certain extent, the utilization efficiency of the CSP system is reduced; the integration of PV and CSP system not only can reduce the power generation cost of CSP system but also can ensure the stability of the output of PV system.

When the output power is set to 95% of the sum of the PV-rated output power and the CSP-rated output power, the system is optimized by the operation characteristics of Spring Equinox and the result is as follows: the lowest LCOE is 0.0660 $/kWh, the capacity of PV and CSP system are 222.462 MW and 30 MW, respectively, and the capacity of heat storage and battery are 356.562 MWh and 14.687 MWh. According to the calculation results, annual power generation of the CSP-PV hybrid system is 368722 MW. Where the annual power generation of PV system is 288291 MW, annual utilization hours are 3261 h, and annual power generation of CSP system is 80431 MW, annual utilization hours are 2681 h.

When the system is optimized by the operation characteristics of the whole year, the result is that the lowest LCOE is 0.0555 $/kWh, the capacity of PV and CSP system are 242.954 MW and 30 MW, respectively, and the capacity of heat storage and battery are 136.059 MWh and 8.977 MWh.

According to the calculation results, annual power generation of PV system is 309036 MW, annual utilization hours are 3201 h, and annual power generation of the CSP system is 66659 MW, annual utilization hours are 2222 h.

The comparison shows that the power generation curves of the hybrid system are similar in the two optimization methods, but LCOE is lower when optimized by the annual operation characteristic, and the annual utilization rate of the system is higher when optimized by Spring Equinox.

The use of optimized CSP-PV hybrid system, which CSP system is to make up for the output power fluctuations of PV systems, can be combined with the advantages of both systems to increase annual operating hours of PV systems to reduce the rate of discards and decrease LCOE of the system but also can guarantee stable output. The operation strategy proposed in this paper provides a new idea for the operation of CSP-PV hybrid power generation system. The optimization method can be used in the preliminary design of power station.

Nomenclature

PV: Photovoltaic
CSP: Concentrated solar power
LCOE: Levelized cost of energy
DC: Direct current
AC: Alternating current
MPPT: Maximum power point tracking
DNI: Direct normal irradiation
GHI: Global horizontal irradiance
T_C: Operating temperature of PV panels
T_A: Ambient temperature
U_L: Actual heat transfer factor
$U_{L,\mathrm{NOCT}}$: Rated heat transfer factor
η_{PV}: Actual PV panel efficiency
$\tau\alpha$: Transfer absorption factor
γ: Temperature factor
$T_{C,\mathrm{REF}}$: PV module temperature under standard test conditions
n_{MOD}: Number of PV subarray
A_{MOD}: Active area of each PV module
η_{INV}: Inverter efficiency
f_{PV}: Derating factor
η_{BC}: Battery efficiencies during charge processes
η_{BD}: Battery efficiencies during discharge processes
SOC: State of charge
DOD: Depth-of-discharge
T_{i}: Inlet temperature of the heat transfer oil
T_{O}: Outlet temperature of the heat transfer oil
ΔT: Temperature difference between the average temperature of the collector field and the ambient temperature
$W_{\mathrm{min,turb}}$: Minimum output of turbine
W_{set}: Rated output of the hybrid system
W_{CSP}: Real output of CSP system
W_{PV}: Real output of PV system
BESS: Battery Energy Storage System
$\mathrm{IC}_{\mathrm{CSP}}$: Initial investment of CSP power station
$\mathrm{IC}_{\mathrm{PV}}$: Initial investment of PV power station
$\mathrm{AC}_{\mathrm{CSP}}$: Annual cost of CSP power station
$\mathrm{AC}_{\mathrm{PV}}$: Annual cost of PV power station
E_{CSP}: Output power of CSP system
E_{PV}: Output power of PV system
d_{CSP}: Annual decay rate of CSP power generation
d_{PV}: Annual decay rate of PV power generation
i: Interest rate
N: Lifetime of system
O&M: Operation and maintain.

Data Availability

The data used to support the findings of this study are available from the corresponding author upon request.

Conflicts of Interest

The authors declare that they have no conflicts of interest.

Acknowledgments

The research work is supported by the National Major Fundamental Research Program of China (No. 2015CB251505) and the Fundamental Research Funds for the Central Universities (2018ZD04, 2016YQ04).

References

[1] Agency, International Energy, *World Energy Outlook 2013*, IEA, Paris, 2013.

[2] J. Spelling, *Solar Power Technologies - Solar Fundamentals*, KTH, Stockholm, 2012.

[3] H. Ibrahim, A. Ilinca, and J. Perron, "Energy storage systems—characteristics and comparisons," *Renewable and Sustainable Energy Reviews*, vol. 12, no. 5, pp. 1221–1250, 2008.

[4] M. Huber, D. Dimkova, and T. Hamacher, "Integration of wind and solar power in Europe: assessment of flexibility requirements," *Energy*, vol. 69, pp. 236–246, 2014.

[5] U. Desideri, F. Zepparelli, V. Morettini, and E. Garroni, "Comparative analysis of concentrating solar power and photovoltaic technologies: technical and environmental evaluations," *Applied Energy*, vol. 102, pp. 765–784, 2013.

[6] Technology Roadmap, *Solar Photovoltaic Energy*, International Energy Agency, Paris, 2014.

[7] IEA, *Solar Energy Perspectives*, IEA, Paris, 2011.

[8] Technology Roadmap, *Solar Thermal Energy*, International Energy Agency, Paris, 2014.

[9] C. Parrado, A. Girard, F. Simon, and E. Fuentealba, "2050 LCOE (Levelized Cost of Energy) projection for a hybrid PV (photovoltaic)-CSP (concentrated solar power) plant in the Atacama Desert, Chile," *Energy*, vol. 94, pp. 422–430, 2016,.

[10] F. Dominio, *Techno-Economic Analysis of Hybrid PV-CSP Power Plants: Advantages and disadvantages of intermediate and peak load operation*, Universitat Politècnica de Catalunya, 2014.

[11] D. Cocco, L. Migliari, and M. Petrollese, "A hybrid CSP–CPV system for improving the dispatchability of solar power plants," *Energy Conversion and Management*, vol. 114, pp. 312–323, 2016.

[12] G. Cau, D. Cocco, and M. Petrollese, "Optimal energy management strategy for CSP-CPV integrated power plants with energy storage," in *Proceedings of the 28th International Conference on Efficiency, Cost, Optimization, Simulation and Environmental Impact of Energy Systems*, Pau, France, 2015.

[13] A. Green, C. Diep, R. Dunn, and J. Dent, "High capacity factor CSP-PV hybrid systems," *Energy Procedia*, vol. 69, pp. 2049–2059, 2015.

[14] M. Hlusiak, M. Götz, and H. A. B. Díaz, "Hybrid photovoltaic (PV)-concentrated solar thermal power (CSP) power plants: modelling, simulation and economics," in *Proceedings of the 29th European Photovoltaic Solar Energy Conference and Exhibition*, Amsterdam, Netherlands, September 2014.

[15] J. P. N. Bootello, S. V. Rubia, L. S. Gallar, and L. F. CAlderon, "Manageable hybrid plant using photovoltaic and solar thermal technology and associated operating method," 2015, U.S. Patent 9140241B.

[16] K. Larchet, *Solar PV-CSP Hybridisation for Baseload Generation: A Techno-economic Analysis for the Chilean Market*, 2015.

[17] L. R. Castillo Ochoa, "Techno-economic analysis of combined hybrid concentrating solar and photovoltaic power plants: a case study for optimizing solar energy integration into the South African electricity grid," 2014.

[18] "Mathworks," June 2018, https://ww2.mathworks.cn.

[19] "System Advisor Model (SAM)," June 2018, https://sam.nrel.gov/.

[20] "Weather data of System Advisor Model," August 2017, https://sam.nrel.gov/weather/.

[21] M. Petrollese and D. Cocco, "Optimal design of a hybrid CSP-PV plant for achieving the full dispatchability of solar energy power plants," *Solar Energy*, vol. 137, pp. 477–489, 2016.

[22] A. M. Patnode, *Simulation and performance evaluation of parabolic trough solar power plants*, University of Wisconsin-Madison, 2006.

[23] S. Shijin, *Simulation and Calculation of Trough Solar Thermal Power Generation*, Inner Mongolia University of Technology, 2014.

[24] H. Suyi and H. Shuhong, *Principle and Technology of Solar Thermal Power Generation*, vol. 204, China Electric Power Press, Beijing, 2012.

[25] R. L. Bartlett, *Steam Turbine Performance and Economics*, McGraw-Hill, New York, 1958.

[26] R. Messenger, J. Ventre, and T. R. Mancini, "Solar electric systems," in *The Engineering Handbook*, CRC Press, Second edition, 2004.

[27] Q. Yin, W. J. Du, and L. Cheng, "Optimization design of heat recovery systems on rotary kilns using genetic algorithms," *Applied Energy*, vol. 202, pp. 153–168, 2017.

[28] T. Gentils, L. Wang, and A. Kolios, "Integrated structural optimisation of offshore wind turbine support structures based on finite element analysis and genetic algorithm," *Applied Energy*, vol. 199, pp. 187–204, 2017.

[29] F. F. Li and J. Qiu, "Multi-objective optimization for integrated hydro–photovoltaic power system," *Applied Energy*, vol. 167, pp. 377–384, 2016.

[30] G. B. Leyland, "Multi-objective optimisation applied to industrial energy problems," in *Section De Génie Mécanique Pour L'obtention Du Grade De Docteur Ès Sciences Techniques par Master of Engineering in Mechanical Engineering*, University of Auckland, 2002.

[31] A. R. Starke, J. M. Cardemil, R. A. Escobar, and S. Colle, "Assessing the performance of hybrid CSP+ PV plants in northern Chile," *Solar Energy*, vol. 138, pp. 88–97, 2016.

[32] S. Ong, C. Campbell, P. Denholm, R. Margolis, and G. Heath, *Land-Use Requirements for Solar Power Plants in the United States*, vol. 140, National Renewable Energy Laboratory, Golden, CO, USA, 2013.